Sub-second striatal dopamine dynamics assessed by simultaneous fast-scan cyclic voltammetry and fluorescence biosensor

Armando G. Salinas[1,2,7,†], Jeong O. Lee[1,†], Shana M. Augustin[1,8], Shiliang Zhang[3], Tommaso Patriarchi[4,5], Lin Tian[4], Marisela Morales[6], Yolanda Mateo[1], David M. Lovinger[1*]

1, Laboratory for Integrative Neuroscience, National Institute on Alcohol Abuse and Alcoholism, National Institutes of Health, Rockville, MD, USA

2, Department of Bioengineering, George Mason University, Fairfax, VA, USA

3, Confocal and Electron Microscopy Core, National Institute on Drug Abuse, Baltimore, MD, USA

4, Department of Biochemistry and Molecular Medicine, University of California at Davis, Davis, CA, USA

5, Institute of Pharmacology and Toxicology, University of Zurich, Zurich, Switzerland

6, Neuronal Networks Section, Integrative Neuroscience Research Branch, National Institute on Drug Abuse, Baltimore, MD, USA

7, Current affiliation, Department of Pharmacology, Toxicology & Neuroscience, Louisiana State University Health Sciences Center – Shreveport, Shreveport, LA, USA

8, Current affiliation, Department of Pharmacology, Northwestern University Feinberg School of Medicine, Chicago, Illinois, USA

† equal contribution

* corresponding author, lovindav@mail.nih.gov

Abstract

Fast-scan cyclic voltammetry (FSCV) is an electrochemical method used to detect dopamine on a subsecond time scale. Recordings using FSCV in freely behaving animals revolutionized the study of behaviors associated with motivation and learning. Despite this advance, FSCV cannot distinguish between catecholamines, which limits its use to brain regions where dopamine is the predominant neurotransmitter. It has also been difficult to detect dopamine *in vivo* in some striatal subregions with FSCV. Recently, fluorescent biosensors for dopamine were developed, allowing for discrimination between catecholamines. However, the performance of these biosensors relative to FSCV has not been determined. Thus, we compared fluorescent photometry responses of the dopamine biosensor, dLight, with FSCV. We also used dLight photometry to assess changes in tonic and phasic dopamine, which has not been possible with FSCV. Finally, we examined dopamine dynamics during Pavlovian conditioning in striatal subregions, including the dorsolateral striatum where dopamine measurements are challenging with FSCV.

Introduction

Dopamine is a catecholamine neurotransmitter found throughout the cortico-mesolimbic circuit of primates and rodents with critical roles in many psychological and neurological disorders including Parkinson's Disease, psychosis, schizophrenia, and addiction (Nestler and Carlezon, 2006; Calabresi et al., 2009; Grace, 2016; Berke, 2018; Ott and Nieder, 2019). Historically, dopamine release has primarily been measured in the brain with either microdialysis sampling coupled with electrochemical detection or fast-scan cyclic voltammetry (FSCV). With the microdialysis technique, measurements of neurotransmitter efflux can be made and specific neurotransmitters chemically identified. Thus, microdialysis allows for precise chemical detection and concurrent measurements of multiple neurotransmitters from each sample (Chefer et al., 2009). However, the major limitation of this technique is the relatively slow sampling time, typically 5-20 minutes per sample. This time scale does not allow for precise correlation of dopamine levels with discrete behavioral events. Fast-scan cyclic voltammetry is an electrochemical method that can be used to measure phasic release of catecholamines (Venton and Cao, 2020). The sampling rates for FSCV are typically set to 10Hz, though faster sampling is possible. Thus, when performed in awake behaving animals, FSCV is used to detect subsecond changes in neurotransmitter release in response to behavioral events. However, FSCV has several limitations. The probes have a finite lifetime and can typically only be used for a handful of sessions, it is a subtractive technique (so measurement of absolute or tonic levels is not possible), and, most importantly, FSCV cannot distinguish between catecholamine neurotransmitters. Thus, FSCV studies of dopamine have focused primarily on the striatum where levels of dopamine far exceed those of noradrenaline. Furthermore, only a few studies have reported *in vivo* FSCV measurements of dopamine levels in the dorsolateral striatum (DLS), especially in mice. This is presumably due to difficulties in detecting small changes sometimes contaminated by other electrochemical signals (e.g. changes in pH). Nonetheless, the major advancement of real-time dopamine measurements in freely behaving animals revolutionized the study of motivated behaviors for well over a decade.

Genetically encoded fluorescent biosensors for dopamine were recently developed (Patriarchi et al., 2018; Sun et al., 2018). These membrane-targeted, G-protein-coupled receptor (GPCR)-based sensors employ modified dopamine receptors that have had a circular permuted Green Fluorescence Protein (cpGFP) molecule replace the third intracellular loop. Upon dopamine binding to the sensor, conformational changes ensue resulting in increased cpGFP fluorescence intensity. Like FSCV, these sensors allow for subsecond sampling times. Although fluorescent dopamine sensors have a similar limitation in measuring absolute concentrations of dopamine, they can detect relative changes in slow (or tonic) modulation, as well as fast (or phasic) dynamics, of dopamine activity within a session. The major advantage of these fluorescent dopamine sensors over FSCV is the chemical specificity and the level of detection. This allows for the real-time measurement of dopamine dynamics in brain regions not previously possible such as in cortex.

As with the introduction of any new method that is based on fundamentally distinct physical and physiological principles, careful consideration of its advantages and limitations should be compared with those of existing methods. Here, we directly compared the photometric measurements employing the fluorescent dopamine sensor, dLight, with FSCV in dorsal striatal brain slices. Measurement with dLight allowed us to detect increases in dopamine at lower stimulus intensities relative to simultaneous FSCV, while the upper end of the dynamic range was

greater with FSCV. We found many similarities in indices of regulation of dopamine release using both methods. However, we noted consistent experimental differences in cocaine-induced effects on dorsal striatal dopamine release that challenge the tacitly accepted, but controversial, notion that cocaine enhances dopamine release *in vitro*. Using pharmacological inhibition of the dopamine transporter (DAT) and electron microscopy (EM) assessment of fluorescent sensor trafficking, we inferred the two measurement systems could have distinctive sensing (and responding) characteristics to identical synaptic dopamine overflow. This led us to suggest a new conceptual model of DAT inhibitor effects on striatal dopamine release, reconciling the methodological discrepancy. Next, we examined striatal dopamine dynamics using *in vivo* fiber photometry with dLight to assess tonic and spontaneous phasic changes in dopamine release in DLS, which is not currently possible with FSCV. In a Pavlovian task for a natural food reinforcer, we also found distinct characteristics of phasic dopamine dynamics in DLS compared to other striatal subregions. This may promote further physiological and behavioral studies in striatal dopamine dynamics.

Results

Direct comparison of simultaneous dLight and FSCV dopamine responses

To directly compare dLight photometry and FSCV, we performed simultaneous recordings using a PMT based photometer and traditional FSCV in the same preparation (Figure 1a). We then collected electrically evoked fluorescence transients from dorsal striatum and found that the fluorescent signals were sensitive to D1 dopamine receptor antagonism (Figure 1b), suggesting that the fluorescence transients arose from the dLight biosensor. When comparing electrically-evoked dopamine release with dLight photometry and FSCV, we found that at lower stimulation intensities dLight responses were apparent when FSCV responses were not (significant main effects of method ($n=7$ slices/5 mice, $p<0.01$, $F(1,12)=11.44$) and stimulation intensity ($p<0.001$, $F(1.645,19.74)=48.17$). Conversely, we also noted that at higher stimulation intensities the dLight signal had plateaued while the FSCV signal remained in its dynamic range (Figure 1c).

dLight fluorescence signals and FSCV originate from dopamine neurons and are dynamic

To ensure that the electrically evoked dLight fluorescence transients were attributable to dopamine release, we used a viral strategy to genetically ablate substantia nigra dopamine neurons. We infused a Cre-dependent Caspase3-encoding virus into the substantia nigra and dLight virus into the dorsal striatum of DAT Cre mice (Figure 1d). At least five weeks later, brain slices were prepared and simultaneous dLight and FSCV recordings were conducted. We found that genetic ablation of nigral DA neurons resulted in significantly reduced dopamine release in DAT Cre+ relative to DAT Cre- mice, as measured with dLight (*, $p<0.05$, $F(1,14)=5.257$) and FSCV (*, $p<0.05$, $F(1,7)=7.63$) across several stimulation intensities Figure 1e & f).

We next assessed whether dLight and FSCV signals would show similar dynamics during manipulations that decrease or increase dopamine release. Thus, we applied the D2 dopamine receptor agonist, quinpirole, to slices to inhibit dopamine release (via activation of presynaptic D2 dopamine autoreceptors). We found that 30 nM quinpirole inhibited dopamine release equally with both methods (Figure 1h; $t=2.032$; $p=0.076$, $df=8$). Having shown that dLight signals could be decreased we assessed whether they could be increased by increasing extracellular calcium levels, which would enhance dopamine release. Indeed, increasing extracellular calcium increased dLight fluorescent responses (Figure 1i & j; *, $p<0.05$, $t=2.611$, $df=12$) demonstrating

that dLight signals are truly dynamic. Further, these results demonstrate similarities in dLight photometry and FSCV dopamine measurements.

Differential regulation of dLight photometry and FSCV dopamine signals by DAT inhibitors

There have been many reports of dopamine transporter (DAT) inhibitor-mediated increases in DA release published using FSCV. However, in Patriarchi et al. (2018), it appeared that cocaine did not increase the dLight dopamine transient peak height. This intriguing observation directly conflicted with a large body of literature and prompted us to directly compare dLight photometry and FSCV dopamine measurements so that we might resolve this methodological discrepancy. We began by comparing the effect of increasing cocaine concentrations on simultaneously collected dLight photometry and FSCV measurements (Figure 2a). We found that cocaine increased the peak amplitude of transients measured with FSCV, but not those measured with dLight photometry (Figure 2b & c). Cocaine increased the duration of both dLight photometry- and FSCV-measured transients, suggesting that cocaine was in fact inhibiting the DAT. We followed up by confirming these results using the more specific DAT inhibitor, nomifensine (1 μM). Similar to cocaine, nomifensine increased the peak transient amplitude measured with FSCV, but not that measured with dLight photometry. Application of nomifensine increased the transient decay time measured with both techniques (Figure 2d).

DAT inhibitors do not affect dopamine release in DAT KO mice

FSCV has been used extensively to study the effects of cocaine and other uptake blockers on the dynamics of dopamine clearance and evoked release. Indeed, to explain how inhibition of the DAT might lead to increased dopamine release (as measured with FSCV), it was posited that cocaine acted via a DAT-independent mechanism (Venton et al., 2006). To evaluate this hypothesis, we again performed simultaneous dLight photometry and FSCV recordings before and after application of cocaine to dorsal striatum brain slices from DAT KO mouse expressing dLight (Figure 2e). In DAT KO mice, the duration of stimulation-induced dopamine transients is prolonged compared to WT mice with a decay in the 10s of seconds, compared 1-2s in WT mice (Jones et al., 1998; Budygin et al., 2002; Mateo et al., 2004). Accordingly, in our experiments, both dLight photometry and FSCV evoked dopamine transients were prolonged relative to WT mice (Figure 2e). In addition, cocaine did not affect either dopamine transient amplitude or decay time using voltammetry (Budygin et al., 2002) or dLight photometry. If the putative cocaine-induced increases in dopamine release assessed with FSCV are due to DAT-independent mechanisms, then the increase in FSCV dopamine transient peak height should be present in DAT KO mice. Since this was not the case, we explored other potential mechanisms for the putative DAT inhibitor-induced increases in FSCV dopamine release.

Altering FSCV adsorption altered DAT inhibitor effects on dopamine release

To further test whether DAT inhibitors increased dopamine release, we decreased the adsorption properties of the FSCV probes by changing the amplitude of the triangle voltage wave form to peak at +1.0V instead of +1.2V. (Figure 2f) (Budygin et al., 2002) to effectively decrease the sensitivity of the FSCV carbon fiber microelectrodes (CFE). Changing the probe sensitivity should not affect detection of putative DAT inhibitor-mediated increases in dopamine release but might reveal if the increase is a function of probe sensitivity. When we assessed evoked dopamine release before and after application of nomifensine (1 μM) using the modified FSCV triangle waveform we found that DAT inhibition increased dopamine transient duration. However, we did not observe significant increases in dopamine transient amplitude with either the modified FSCV protocol or dLight photometry (Figure 2g & h).

DAT inhibitors do not increase dopamine release: a new model to reconcile methodological differences

To reconcile these results, we posited a new model for the effects of DAT inhibitors on dopamine transients measured with FSCV (Figure 2i). The detection of dopamine with FSCV relies on the electrochemical oxidation of dopamine at the surface of the CFE. Upon electrical stimulation of the slice, dopamine is released and diffuses across a given volume. The extent of this diffusion is determined by several factors but most notably DAT (Venton et al., 2003; Cragg and Rice, 2004). Thus, in a given space, the sampling volume obtained with FSCV is limited to the distance that dopamine can diffuse to the CFE surface. Under conditions of impaired DAT function, however, the diffusion distance of dopamine increases. This increased release point diffusion of dopamine also increases the effective sampling volume of the CFE, resulting in a larger signal, but not increased release per se.

dLight sensor traffics to synaptic and extrasynaptic sites

We next sought to determine if dLight could traffic to synaptic sites. This would mark a major advance in the measurement of dopamine as both microdialysis and FSCV can only measure non-synaptic dopamine overflow. We performed immunohistochemistry for tyrosine hydroxylase (TH), the rate limiting step in catecholamine synthesis and GFP to label dLight in mouse dorsal striatum. We found putative dopamine axons (i.e. TH+ axons) juxtaposed to dLight/GFP (Figure 3a), suggesting the possibility of dLight expression in proximity to dopamine release sites. We followed up these experiments with electron microscopy (EM) experiments to directly assess whether dLight would traffic to synapses and thus, at least partially, report synaptic dopamine release. We found that dLight trafficked exclusively to plasma membrane (Figure 3b) or membrane-associated regions within the cell (Figure 3c). We also found that dLight could indeed traffic to synaptic sites, including putative dopamine synapses (Figure 3d).

dLight allows for measurements of tonic and phasic dopamine release *in vivo*

We next determined whether dLight could be used to address limitations of microdialysis and FSCV. For example, while tonic dopamine level measurements are possible with microdialysis, they are not possible with FSCV. In contrast, FSCV, but not microdialysis, allows for measurements of phasic dopamine release. We thus explored the utility of dLight to assess both tonic and phasic changes in dopamine release *in vivo* by designing an experiment in which both parameters change. We expressed dLight in dorsolateral striatum (DLS) and measured fluorescence intensity profile using a custom-built, sensitive *in vivo* fiber photometry system based on time-correlated single photon counting (TCSPC) principles (schematic in Figure 4a). Using this system, we measured dLight fluorescence from the DLS before and after administration of cocaine (15 mg/kg i.p.). We found that cocaine increased tonic dopamine levels within the behavioral session (Figures 4b and c). When we examined phasic changes, we observed dopamine transients before and after cocaine administration (Figure 4d). To examine the profiles of these spontaneous transients before and after cocaine administration, we time-locked the transients to their peaks (Figure 4e & f). We then analyzed cocaine-induced changes in transient frequency, amplitude, and decay (Figure 4g-j). We found that cocaine increased dopamine transient frequency ($t=4.887$, $p<0.001$, $df=16$) and amplitude ($t=13.81$, $p<0.001$, $df=16$). Furthermore, we found that cocaine increased the decay time constant of spontaneous dopamine transients ($t=4.730$ $p<0.001$, $df=79$).

Measured in vivo changes in fluorescence originate from dLight

To ensure that our observed changes in fluorescence originated from dLight (and not blood flow, for example), we treated mice with the D1 dopamine receptor antagonist SCH23390 to block the dLight sensor. Indeed, treatment with SCH23390 eliminated phasic dopamine transients (Figure 4k). Further, in the presence of SCH23390, the fluorescence profile for dLight resembled that of a static eGFP control mouse.

In vivo DA dynamics across striatal regions during Pavlovian conditioning

We next compared dLight responses throughout training on a Pavlovian task across striatal subregions (dorsomedial striatum [DMS], DLS, and nucleus accumbens [NAc]) with published FSCV results. We trained animals in a well-established conditioning paradigm for a food reinforcer and compared the dopamine responses across regions (Figure 5a & b). Pavlovian responding was consistent with previous reports as mice learned to associate the presence of a food reinforcer with a cue (CS+). Dopamine transients evoked by the CS+ were compared across the striatal subregions. We found that the average decay time decreased across the striatum in a ventromedial to dorsolateral gradient such that the decay times in DLS were significantly faster than in NAc (Figure 5d & e; one-way ANOVA, $F(2,27)=14.93$, $p<0.0001$). Furthermore, we found that dopamine transient amplitudes tied to the CS+ were generally larger in amplitude in the NAc in comparison to other striatal subregions. Similar to previous work (Brown et al., 2011; Willuhn et al., 2012; Patriarchi et al., 2018), we observed dopamine transients tied to the reinforcer delivery that gradually shifted to the presentation of the CS+ in all three striatal subregions (Figure 5f). Interestingly, in the DMS and DLS, a transient response to the reinforcer delivery remained late in conditioning. Of note, in the DMS and DLS, we observed no dopamine transients in response to the CS- and a relatively smaller response to the CS- in the NAc. Since we used auditory cues for both the CS+ and CS- we believe some generalization to an auditory stimulus may have occurred in our NAc mice. Across 10 weeks of training, we observed an increase in the average amplitude of the CS+ associated dopamine increases (Figure 5h) and stable reward associated dopamine increases (Figure 5i).

Discussion

Summary of findings

This is the first study to directly and simultaneously compare dLight photometry with FSCV in vitro. To our knowledge, this is also the first study to demonstrate both cocaine-induced tonic and phasic changes in dopamine in the dorsal striatum *in vivo*.

In comparing dLight and FSCV signals, we note several similarities and some notable differences. We found that electrical stimulation at low intensities (<100 μA) could evoked dLight fluorescence signals that were not detectable with FSCV. We also found that the dLight signal was maximal at mid and higher stimulation intensities (>400 μA) sometimes used in FSCV. To determine if the electrical stimulation-induced changes in fluorescence we observed were indeed due to dLight, we applied a D1R antagonist and blocked the fluorescence responses. Our observation that transients are reduced following virally expressed Caspase3 ablation of DAT Cre+ substantia nigra neurons supports the idea that transients measured with either dLight photometry or FSCV are mediated by dopamine release from these neurons. Thus, we concluded

that the electrical stimulation induced changes in fluorescence were due to dopamine terminal-induced activation of the dLight sensor. We next sought to determine if regulation of dopamine release by the D2 autoreceptor would be similar when comparing the two methods and found that application of 30 quinpirole (D2 dopamine receptor agonist) resulted in a similar average inhibition of evoked dopamine release measured with both techniques.

"Sensitivity" differences between dLight photometry and FSCV

We found that the dynamic range of dLight fluorescent responses to electrical stimulation was left-shifted relative to voltammetric responses collected in the same preparation. Indeed, evoked photometric responses were nearly saturated by stimulation intensities yielding a ~50% maximal voltammetric response. This could be interpreted to mean that dLight responses are more "sensitive" than voltammetric responses, however, this may be an oversimplification. Comparisons of sensitivity should account for differences in sampling volume to yield a response value per unit of measurement (e.g. 5% dF/F or 500nM DA per μm^3). Thus, the fundamentally different sampling volumes for each method preclude statements about direct differences in sensitivity. Nonetheless, the inherently greater sampling volumes in *in vivo* and *in vitro* photometric methods facilitate the detection of dopamine (or any "volume" neurotransmitter) in a way that is not possible with single electrode voltammetric methods.

Tonic vs phasic dopamine

Striatal (and likely extra-striatal) dopamine operates on multiple time scales and dopamine levels include tonic and phasic components (Liu et al., 2021). Tonic, or basal, dopamine levels are set by the basal firing rate of midbrain dopamine neurons and possibly modulated by local striatal mechanisms. Changes in tonic dopamine are typically slow and sustained. In contrast, phasic dopamine changes are faster, typically lasting on the order of seconds, and are mediated by burst firing of midbrain dopamine neurons, local control of dopamine release (e.g. by acetylcholine or glutamate receptors on dopamine axons), or both (Zhou et al., 2001; Cachope et al., 2012; Threlfell et al., 2012). Tonic and phasic dopamine play distinct roles in behavior and motivation (Beeler et al., 2010; Hamid et al., 2016; Berke, 2018; Mohebi et al., 2019; Wang et al., 2021). Microdialysis sampling with electrochemical detection techniques allow for assessment of tonic dopamine levels within and between test sessions but cannot be used to assess phasic changes in dopamine levels on a behaviorally-relevant time scale. In contrast, the subsecond sampling in FSCV allows for measurement of phasic dopamine levels but due to the subtractive nature of the method, it cannot be used to determine changes in tonic dopamine levels. Given these limitations, dLight (and other fluorescent biosensors) represents a technological advance. As we demonstrate here, dLight allows for the assessment of both tonic and phasic dopamine release within an *in vivo* testing session (Figure 4). This was evident in our experiments examining the effect of acute cocaine treatment on dorsolateral striatum dopamine release where we observed an increase in tonic dopamine levels following cocaine administration as well as an increase in phasic dopamine transient amplitude, frequency, and duration. In contrast to our *in vitro* work, we observed a cocaine-induced increase in transient amplitude *in vivo*. This is likely due to the slower sampling rates used for our *in vivo* recordings (20 Hz) which may be too slow to capture the phasic or burst firing frequencies of dopamine neurons (up to 100Hz) which are thought to underlie phasic dopamine transients (Hyland et al., 2002; Lohani et al., 2018). Indirect

cocaine effects may also contribute to increased transient amplitudes in vivo. For example, cocaine could alter midbrain dopaminergic neuron firing in vivo, and this could also contribute to transient amplitudes (Covey et al., 2014). Such effects would not contribute to dopamine release in brain slices.

An understanding of the significance of tonic and phasic dopamine is important. Changes in phasic dopamine release can occur without changes in tonic dopamine levels and vice versa. Also, tonic levels may serve to influence global striatal activity or metaplasticity. For example, a low tonic dopamine level may preferentially activate the higher affinity D2-like dopamine receptors. Conversely, at higher tonic dopamine levels, recruitment of D1-like dopamine receptors may occur (Richfield et al., 1989; Martel and Gatti McArthur, 2020). This difference in neuromodulation can influence synaptic activity. For example, the chronic DA deficiency observed in PD models is often accompanied by changes in synaptic plasticity or altered cellular physiology (Calabresi et al., 2009; Surmeier et al., 2014; Wang and Zhang, 2016; Zhai et al., 2018; Graves and Surmeier, 2019). Thus, the ability to simultaneously assess tonic and phasic changes in dopamine release in freely-behaving animals represents a tremendous advance for the field.

Technical considerations for sampling

Sampling rates can be much faster with photometry than with FSCV. FSCV sampling is inherently limited by the electrochemical properties of the triangle wave form (~8ms) and the time required for desorption of dopamine from the CFE surface, resulting in a maximum practical sampling rate of up to ~50Hz (though 10Hz is typical for dopamine measurements). In contrast, the sampling rates for photometric methods are limited by the digitization rate of the data acquisition hardware used. Our *in vitro* photometric responses were collected at 100Hz or 1,000Hz, though up to 20,000Hz is possible with our hardware configuration. *In vivo* fiber photometry sampling rates with most available systems can also be exceed 100Hz. However, given the known time course of dopamine signaling we chose to perform our recordings at 20Hz, which is double the typical sampling rate used in FSCV. It is important to note that, with photometric methods, the fluorescent on/off rates of dLight (or other biosensors) will limit the utility of high sampling rate data. For example, the on and off rates for dLight1.1 are ~10 and 100ms, respectively (Patriarchi et al., 2018; Sabatini and Tian, 2020). Thus, it is possible that sampling at 200Hz with dLight1.1 will yield a large data set that would not differ practically from a data set collected at 100 or even 20Hz. These fluorescence kinetics may also limit interpretation of transient rise times or modeling of decay kinetics as the fluorescent signal may not actually represent the termination of neuromodulator signaling but rather the off rate of the sensor. Thus, consideration of the experimental question and the type of data that can be collected should be considered when choosing a fluorescent biosensor (Labouesse et al., 2020; Sabatini and Tian, 2020).

Synaptic dopamine vs overflow

Using dLight it may be possible to assess truly “synaptic” dopamine release. That is to say, both microdialysis and FSCV are methods that measure dopamine overflow out of the synapse. Because of the size of the probes, sampling of dopamine at synaptic release sites has not been possible with either of these methods. In this context, dLight represents another major

advance for the field because it can be genetically targeted to distinct cellular compartments. For example, dLight sensors are integral membraine proteins so they will only be expressed in membranes. We confirmed this with our electron microscopy work and show that indeed, dLight traffics strongly to plasma membrane, Golgi, and ER compartments of the neuron (Figure 3c). Further, our results show that dLight traffics to synaptic and extrasynaptic sites (Figure 3b,d). Thus, dLight signals likely represent dopamine release at synaptic and extrasynaptic sites. Work from the Ford and Williams labs (Ford et al., 2009; Marcott et al., 2014; Mamaligas et al., 2016) utilized an indirect electrophysiological approach to measure GIRK-mediated currents activated by D2 dopamine receptors. However, like the dLight method we used, this approach likely represents a mixture of synaptic and extrasynaptic dopamine release. More recent work from the Williams lab used two photon excitation with dLight to measure dopamine release at spatially discrete sites in the midbrain (Condon et al., 2021). Given the sparsity of dopamine release sites in midbrain, it is possible that these spatially discrete sites represent dopamine synapses. Thus, the use of dLight with high resolution imaging methods may allow for measurement of synaptic dopamine release. Furthermore, with dual color fluorescence imaging methods, synaptic markers could be employed to allow for labeling of pre- or post-synaptic elements to colocalize with dLight (or other biosensor) signals, facilitating measurement of truly synaptic neuromodulator release.

A new method settles an old controversy

Pharmacologically, the direct mechanism of action of cocaine is inhibition of the DAT (and other monoamine transporters). This should result in prolonged phasic dopamine transients and, in regions where the primary mechanism of dopamine clearance is the DAT, increases in tonic dopamine levels. Indeed, with microdialysis, the expected increases in tonic dopamine have been confirmed (Church et al., 1987; Hurd et al., 1988). With FSCV, the duration of evoked dopamine transients is increased. Interestingly, with FSCV, cocaine (and other DAT blockers) also increases the observed dopamine transient peak amplitude in brain slices. This is often interpreted to mean that DAT blockers enhance or facilitate electrically evoked dopamine release in slice. From a pharmacological perspective, this is not intuitive as dopamine release should not be affected by DAT inhibition. Interestingly, Patriarchi et al. (2018) noted that there was no increase in dLight dopamine transient peak amplitude in response to cocaine application. Following up on this, we performed simultaneous dLight and FSCV recordings in the same preparation to compare the cocaine effect on dopamine transient peak amplitude and transient duration. Similar to previous work, we observed a large cocaine-induced increase in dopamine transient peak amplitude with FSCV but only modest or no effects with dLight (Figure 2). With both methods, the dopamine transient decay was prolonged. We repeated these experiments with the more specific DAT blocker nomifensine and observed similar results. To examine this discrepancy, we first considered that the physical interaction of dopamine with the carbon fiber electrode may be the culprit. We thus modified the triangle waveform used in typical FSCV to modify the adsorption properties of dopamine to the carbon fiber electrode. This modification resulted in a loss of the nomifensine-induced increases in dopamine transient peak amplitude normally observed in FSCV recordings with the traditional voltage triangle waveform (Figure 2h-j). We posit that if DAT inhibitors did in fact increase dopamine release (Wu et al., 2001; Venton et al., 2006; Oleson et al., 2009; Kile et al., 2010; Yorgason et al., 2011; Covey et al., 2014; Hoffman et al., 2016; Salinas et al., 2016), then the change in CFE sensitivity to dopamine with the modified waveform should not adversely affect putative DAT blocker-induced increases in dopamine release. In a follow up

experiment, we applied cocaine to dorsal striatal brain slices from DAT KO mice. We did not observe any cocaine-induced increase in dopamine release (Figure 2) in DAT KO mice. Our observation that dopamine transients were not prolonged by cocaine in DAT KO mice is consistent with the lack of functional transporter. These findings are in line with previous work in DAT KO mice showing no contribution of other catecholamine transporters to DA clearance in NAc (Budygin et al., 2002; Mateo et al., 2004). Altogether, our data do not support the idea of DAT blocker-induced increases in dopamine release. Therefore, we posit the following alternative interpretation of the observed DAT blocker-induced increases in dopamine transient peaks using FSCV. Rather than increasing or facilitating dopamine release, DAT blockers by virtue of their DAT blockade allow for an increase in the point diffusion of dopamine from its release site. That is to say, under normal conditions, the diffusion of dopamine is limited by several factors, most notably the DAT (Cragg and Rice, 2004; Hoffman et al., 2016) but under conditions of impaired DAT function (e.g. in the presence of a DAT blocker) the diffusional spread of dopamine from its release site is increased (Venton et al., 2003). This would effectively increase the sampling volume of CFEs allowing for greater FSCV detection of dopamine (and increased dopamine transient peak heights) without increasing its release. Further, because the sampling volume used in photometric methods is already much larger than with FSCV methods, the cocaine-induced increase in dopamine diffusion from its release site has a more negligible effect on dLight/photometric DA transients. Thus, we believe that dLight more faithfully reflects dopamine release dynamics than FSCV, especially under conditions where dopamine overflow or uptake may be affected.

dLight allows for insights of striatal subregion dopamine release differences

FSCV has been used to measure dopamine release *in vivo* across the striatum. However, the majority of these studies have focused on the nucleus accumbens where the relative increases in phasic dopamine signal are larger than in dorsal striatum. Few FSCV studies have examined the dorsomedial striatum (DMS) in Pavlovian conditioning and even fewer have examined dopamine dynamics in the dorsolateral striatum (DLS) (Brown et al., 2011; Willuhn et al., 2012). This may be due to the difficulty in obtaining dorsolateral striatum FSCV signals. Here we compared dopamine transients across the three striatal subregions: the NAc, DMS, and DLS. We found that dopamine transient decay times decreased across the striatum in a ventromedial to dorsolateral gradient (Figure 5), reflecting prior *in vitro* findings that showed a similar gradient in dopamine uptake (Calipari et al., 2012) and was suggested *in vivo* (Brown et al., 2011).

The end of FSCV?

dLight photometry has several advantages over FSCV. We have highlighted some of these differences and demonstrated how we used dLight to clarify a controversial finding that resulted from a technical limitation of the FSCV method. Further, we demonstrated the use of in vivo dLight photometry to assess both phasic and tonic changes in dopamine signaling within a single session. Finally, we show that dLight photometry is suitable for use *in vivo* in DLS with a natural food reinforcer (where dopamine recordings have proven challenging with FSCV). An additional benefit of dLight photometry over FSCV is the ability to measure dopamine in brain

regions where the presence of multiple catecholamines (e.g., norepinephrine in cortex) makes FSCV measurements difficult, if not impossible, to interpret. In contrast, the ability to distinguish between neurotransmitters with photometry is limited by the specificity of the GPCR (or other receptor) used to produce the sensor. Along these lines, several new fluorescent biosensors have been developed for neuromodulators like norepinephrine, serotonin, and endocannabinoids (Feng et al., 2019; Unger et al., 2020) and many more fluorescent biosensors for opioids, adenosine, and peptides, to name a few, are in development. All of these sensors will be compatible with the *in vitro* and *in vivo* hardware used for dLight photometry. Finally, different fluorescent biosensors for dopamine (and other neuromodulators) are being developed to allow fluorescent photometry recordings of multiple neuromodulators simultaneously. For example, a red version of dLight (RdLight) was recently introduced and was used alongside a glutamate biosensor *in vitro* and *in vivo* (Patriarchi et al., 2020). Such multiplex fluorescent recordings represent one of the major advances possible with photometric methods that are not currently possible with FSCV.

With clear advantages on several fronts, dLight appears poised to replace FSCV as the method of choice for dopamine measurements. However, despite the advantages of photometric dopamine measurements, there exist several potential limitations. For example, currently, dLight expression is induced with AAV infusion into the brain region of interest. Sufficient expression of dLight to allow for reliable photometric recordings typically takes a minimum of two weeks. This may not be suitable from some experiments that must be performed in animals naïve to any surgeries or that are too young for stereotaxic virus infusions. Furthermore, virus infusions may not be practical in some model systems (e.g. nonhuman primates) due to the large cost and amounts of virus needed. Indeed, FSCV has been used to measure striatal dopamine in the human brain during neurosurgery (Kishida et al., 2011), where recordings with dLight photometry are unlikely to be made any time in the foreseeable future. A more practical consideration for many labs may be the cost to purchase equipment for use in *in vitro* (e.g., sCMOS camera or PMT) or *in vivo* (many turnkey options or custom photometry builds) experiments. Similarly, the cost of fiber optic implants exceeds by several factors those used for *in vivo* FSCV. Thus, it is likely that FSCV will continue to be used, at least on a limited basis, for the measurement of phasic dopamine transients *in vitro* and *in vivo*.

Materials and Methods

Subjects

Three-month-old, male C57BL/6J mice were obtained from the Jackson Laboratory (Strain 000664) and pair-housed in the vivarium for at least one week before any experimental use. DAT-IRES-Cre mice were obtained from the Jackson Laboratory (Strain 006660) and bred in house. DAT KO mice were developed as previously described (Giros et al., 1996) and obtained from the Sara Jones laboratory at Wake Forest University. Male and female DAT-IRES-Cre and DAT KO transgenic mice were used in all experiments. All mice were housed with 2-4 mice per cage and maintained on a 12:12 hour light cycle and ad libitum access to food and water.

All procedures performed in this work follow the guidelines of the Institutional Animal Care and Use Committee of the Division of Intramural Clinical and Biological Research, National Institute on Alcohol Abuse and Alcoholism, and the animal care and use protocol was approved by this committee.

Viruses and Stereotaxic Injections

The Caspase3-coding virus (AAV1-EF1a-FLEX-taCasp3-TEVp) was custom packaged by Vigene Biosciences and a gift from Dr. Huaibin Cai, National Institute on Aging. dLight1.1 viruses were used for *in vitro* experiments and were either generated in the Tian laboratory and sent to NIAAA (AAV5-CAG-dLight1.1 and AAV9-CAG-dLight1.1) or purchased from Addgene (pAAV5-CAG-dLight1.1; Addgene viral prep # 111067-AAV5). dLight1.3b virus was used for *in vivo* experiments and supplied by theTian laboratory or custom packaged by Vigene Biosciences (AAV9-CAG-dLight1.3b).

All stereotaxic injections were conducted using sterile technique on mice at least 3 months of age. Mice were anesthetized with a 5% isoflurane/oxygen mixture and placed in a Kopf stereotaxic frame. Anesthesia was maintained with 1-2% isoflurane/oxygen mixture. The skulls were leveled and an incision was made to expose the skull. Craniotomies were made over the dorsal striatum (AP +1.0, ML +/-1.8, from Bregma in mm), nucleus accumbens (AP +1.2, ML +/-0.8, from Bregma in mm) or substantia nigra (AP -3.0, ML +/-1.2, from Bregma in mm) and a 1 µL Neuros Hamilton Syringe was lowered slowly to the desired depth from the brain surface (-2.25mm, -3.75mm, and -4.1mm for dorsal striatum, nucleus accumbens, and substantia nigra, respectively). Virus infusion volumes were 300nL for dorsal striatum and 500nL for VTA and viruses were infused at 50nL/minute. After infusions were completed, the syringe was left in place for 10 minutes before withdrawal and the incisions were closed with VetBond. Mice recovered for at least three weeks before being used for in vitro experiments or fiber optic implantation for *in vivo* experiments.

Simultaneous Photometry and Voltammetric Recordings

Dual photometric and voltammetric recordings were conducted as previously described (Sgobio et al., 2014; Sgobio et al., 2019) except that the photometry recordings in the current study used dLight1.1 or dLight1.3b to compare dopamine release between voltammetric and photometric methods simultaneously in the same preparation. Brain slices containing the striatum were prepared as previously described (Salinas et al., 2016). Briefly, mice were anesthetized with isoflurane, rapidly decapitated, brains extracted, and 300µm thick coronal sections prepared on a vibratome (Leica VT 1200S). The slices were hemisected and inspected to ensure viral expression of dLight in the region of interest using an epifluorescent Zeiss AxioZoom microscope

equipped with a GFP filter set. Then the slices were incubated at 32°C for 30 minutes before being moved to room temperature for one hour before beginning experiments.

Brain slices with dLight expression were moved to an upright Zeiss AxioSkop2 microscope mounted on a XY translational stage and equipped with a GFP filter set. Oxygenated ACSF was perfused at 1.5-2mL/minute and warmed to 30-32°C. The recording region of interest was located under 4X magnification and fluorescent illumination to ensure dLight expression in the region of interest. Then a stainless steel twisted bipolar stimulating electrode (P1 Technologies) was placed on the tissue surface near the area of dLight expression. For simultaneous photometry-voltammetry recordings, carbon fiber electrodes (CFE) were fabricated as previously described (Salinas et al., 2016; Salinas et al., 2021) and placed in the tissue in the center of the recording region of interest under 4X magnification. Slices were then visualized with 40X objective (0.8 NA) and the field of view (~180um x 180um) was adjusted so the stimulating electrode was just outside the field of view and the CFE was in the center of the field of view. Under 40X magnification, the focus was adjusted to a focal layer beneath the slice surface where fluorescent cells could be identified. Fluorescent transients were quantified with a PMT-based system (PTI D-104 photometer) coupled with a Digidata 1322A (Molecular Devices LLC) to digitize the PMT signal (100-1,000Hz). Clampex software was used to collect photometry data and synchronize photometric and voltammetric recordings through the Digidata. A mechanical shutter (Uniblitz V25) was used to limit exposure to fluorophore-exciting light to discrete periods and minimize photobleaching of the dLight between recordings. FSCV recordings were carried out as previously described (Sgobio et al., 2014; Salinas et al., 2016; Sgobio et al., 2019; Salinas et al., 2021). Briefly, a triangle wave form voltage was applied to the CFE beginning at -0.4V to +1.2V and back to -0.4V. This scan was applied at 400V/s and repeated at 10Hz. Dopamine was identified electrochemically by the oxidation peak at +0.6V on the ascending phase of the triangle ramp. Dopamine release was evoked with electrical stimulation delivered every three minutes using a constant current stimulus isolator (DigiTimer DS3). Input-output (IO) curves were generated to compare method sensitivity to evoked dopamine release across varying electrical stimulation intensities (50-800 µA, 1 ms). For pharmacological experiments, a stimulation intensity yielding approximately 30-60% of the maximal responses with both methods was used to ensure that any subsequent treatments were not limited by floor or ceiling response effects. Baseline responses were collected for 12-20 minutes before drugs (dissolved in ACSF) were bath applied as indicated for each experiment.

In Vivo Fiber Photometry

At least three weeks after virus infusion surgeries, mice used for *in vivo* experiments underwent a second surgery to implant the optical fiber, similar to those previously described (Kupferschmidt et al., 2017). Briefly, mice were anesthetized and mounted into the stereotaxic apparatus and an incision was made in the scalp along the skull midline as before. The skull was cleaned with a 3% H_2O_2 solution to remove any connective tissue and the skull was scored several times with a scalpel to create a better surface for the dental cement headcap at the end of the procedure. Craniotomies were made over the brain region of interest and two distal sites for anchor screw placement. The anchor screws were placed before proceeding to the fiber optic placement. To ensure optimal fiber optic placement, fluorescence intensity was monitored intraoperatively using a custom designed fiber photometry system consisting of a 473 nm picosecond pulsed laser, a HPM-100-40 hybrid detector, and a SPC-130EM time correlated single photon counting (TCSPC) module and software (Becker & Hickl). The measurement rate for the fluorescence lifetime and

intensity profile was set at 20Hz during all animal experiments. The output was a custom multimode patch cord from Thor labs with a 0.22NA and 200µm fiber core diameter terminating in a 2.5mm ceramic ferrule. The patch cord ferrule was connected to the fiber optic cannula (CFMC22L05, Thor Labs) to be implanted with a ceramic mating sleeve. The implantable fiber optic cannula was lowered slowly into the craniotomy over the brain region of interest while the fluorescence intensity at the desired emission wavelengths (~500-540 nm) was monitored. The fluorescence intensity typically increased as the fiber optic approached the area of dLight expression. Once fluorescence intensity plateaued, typically ~300-500µm dorsal to the virus infusion site, the fiber optic cannula was cemented in place and the surgical site was closed around the dental cement headcap. Mice recovered for at least two weeks before further experiments.

For the Pavlovian conditioning experiment, the TCSPC system was synchronized to the operant behavior boxes (MED-PC) through a TTL channel, in which the TTL pulse generated by MED-PC controller was used to trigger the TCSPC system acquisition for 10s prior to each trial (CS+ or CS-) and maintained 60s of data acquisition. The pulsed laser was continuously turned on and sustained stable laser illumination during the entire session. *In vivo* pharmacology measurements were collected in a continuous recording mode at 20Hz without any TTL controls.

Pavlovian Conditioning

At least three weeks following fiber optic implant surgeries, mild food restriction was carried out to gradually reduce the animals' body weight to 85-90% of their initial body weight. Thus, chow was limited to 2–3 g per day for 3 days. Concurrently, mice were handled and tethered to an optical patch cord cable within the designated behavior training time. For the first 2 days of pre-training, mice received habituation sessions in the operant training box for 1-hr while tethered to the optical patch cord. In the final day of pre-training, mice underwent a magazine training session in which 30 food pellets were delivered on a random-interval schedule (RI-60). No stimulus cue was provided during these sessions. After 3 days of food restriction and pre-training, mice underwent Pavlovian conditioning sessions. The discrimination training entailed two conditioned stimuli; one conditioned stimulus (CS+) was a high-frequency auditory cue followed by the US (one 15mg food pellet) as a reinforcer, and a second stimulus (CS-) was a low-frequency auditory cue which was not accompanied by a reinforcer delivery. Within a single session, mice received 20 CS+ trials and 20 CS- trials. In the operant conditioning box within sound and light attenuating enclosures, the auditory cue was presented for 1 second with random intertrial intervals (60-s to 120-sec). In the CS+ trials, an US reinforcer was delivered to a pellet receptacle 1 second after the CS+ cue offset. *In vivo* photometry measurements were conducted every other day during the training, but the mice underwent the same continuous daily Pavlovian training sessions while tethered to an optical patch cord (Thor Labs, 200um core, 3 m length) even if photometry measurements were not conducted. Therefore, DLS and DMS mice received 60-days of consecutive daily Pavlovian training. NAc mice received four weeks of Pavlovian training. All animals received the behavior training with 24 (+/-2) hours of interval at their own designated time, and animals were acclimated to the behavior room for at least 1hr before all training sessions.

Fluorescence microscopy

For anatomical studies, dLight virus injected mice were deeply anesthetized with chloral hydrate (35 mg per 100 g), and perfused transcardially with 4% (wt/vol) paraformaldehyde (PFA) with

0.15% (vol/vol) glutaraldehyde and 15% (vol/vol) picric acid in 0.1 M phosphate buffer (PB, pH 7.3). Brains were left in this fixative solution for 2 h at 4 °C, solution was replaced with 2% PFA and left overnight at 4 °C. Brains were rinsed with PB, and cut into coronal serial sections (40 µm thick) with a vibratome (Leica). All animal procedures were approved by the National Institute on Drug Abuse Animal Care and Use Committee.

Free floating coronal vibratome sections were incubated for 1 h in PB supplemented with 4% bovine serum albumin (BSA) and 0.3% Triton X-100. Sections were then incubated with mouse anti-tyrosine hydroxylase (TH) antibody (1:1,000 dilution, Millipore-Sigma, Cat# MAB318, RRID: AB_2201528) overnight at 4°C. After rinsing 3 × 10 min in PB, sections were incubated in Alexa Fluor 594-affiniPure donkey anti-mouse (1:100 dilution, Jackson Immunoresearch Laboratories, Cat# 715-585-151, RRID: AB_2340855) for 2 h at room temperature. After rinsing, sections were mounted on slides and air-dried. Fluorescent images were collected with Zeiss LSM880 Airyscan Confocal System (Zeiss, White Plains, NY). Images were taken with 20× objectives and z-axis stacks were collected at 1 µm. The confocal images were collected from 3 mice.

Electron microscopy

Vibratome tissue sections were rinsed with PB, incubated with 1% sodium borohydride in PB for 30 min to inactivate free aldehyde groups, rinsed in PB, and then incubated with blocking solution [1% normal goat serum (NGS), 4% BSA in PB supplemented with 0.02% saponin] for 30 min. Sections were then incubated with primary antibody guinea pig anti-GFP (1:500 dilution, Nittobo Medical, Cat# GFP-GP-Af1180, RRID: AB_2571575); or primary antibodies guinea pig anti-GFP (1:500 dilution) and mouse anti-TH (1:1,000 dilution) for 24 h at 4°C. Sections were rinsed and incubated overnight at 4°C in the secondary antibody goat anti-guinea pig IgG Fab fragment coupled to 1.4 nm gold (1:100 dilution for GFP detection; Nanoprobes Inc., Cat# 2055, RRID: AB_2802149); or the corresponding secondary antibodies: biotinylated goat anti-guinea pig antibody (1:100 dilution for GFP detection; Vector Laboratories, Cat# PK-4007; RRID:AB_2336816) and secondary antibody goat anti-mouse IgG coupled to 1.4 nm gold (1:100 dilution for TH detection; Nanoprobes Inc., Cat# 2001, RRID:AB_2877644). Sections were incubated in avidin-biotinylated horseradish peroxidase complex in PB for 2 h at room temperature and washed. Peroxidase activity was detected with 0.025% 3,3′-diaminobenzidine (DAB) and 0.003% H_2O_2 in PB for 5-10 min. Sections were rinsed in PB, and then in double-distilled water, followed by silver enhancement of the gold particles with the Nanoprobe Silver Kit (2012; Nanoprobes Inc., Stony Brook, NY) for 7 min at room temperature. Next, sections were rinsed with PB and fixed with 0.5% osmium tetroxide in PB for 25 min, washed in PB followed by double-distilled water and then contrasted in freshly prepared 1% uranyl acetate for 35 min. Sections were dehydrated through a series of graded alcohols and with propylene oxide. Afterwards, they were flat embedded in Durcupan ACM epoxy resin (14040; Electron Microscopy Sciences, Fort Washington, PA). Resin-embedded sections were polymerized at 60°C for 2 days. Sections of 65 nm were cut from the outer surface of the tissue with an ultramicrotome UC7 (Leica Microsystems Inc., Buffalo Grove, IL) using a diamond knife (Diatome, fort Washington, PA). The sections were collected on formvar-coated single slot grids and counterstained with Reynolds lead citrate. Sections were examined and photographed using a Tecnai G2 12 transmission electron microscope (Fei Company, Hillsboro, OR) equipped with a digital micrograph OneView camera (Gatan Inc., Pleasanton, CA).

Ultrastructural analysis

Serial thin sections of dorsal striatum of the mice were used in this study. Synaptic contacts were classified according to their morphology and immuno-label and photographed at a magnification of 6800-13000×. The morphological criteria used for identification and classification of cellular components observed in these thin sections were as previously described (Zhang et al., 2015). Type I synapses, here referred as asymmetric synapses, were defined by the presence of contiguous synaptic vesicles within the presynaptic axon terminal and a thick postsynaptic density (PSD) greater than 40 nm. Type II synapses, here referred as symmetric synapses, were defined by the presence of contiguous synaptic vesicles within the presynaptic axon terminal and a thin PSD. Serial sections were obtained to determine the type of synapse. In the serial sections, a terminal or dendrite containing greater than 5 immunogold particles were considered as immuno-positive terminal or dendrite. Pictures were adjusted to match contrast and brightness by using Adobe Photoshop (Adobe Systems Incorporated, Seattle, WA). The frequency of gold particles for GFP signals near to asymmetric synapses was counted from 3 mice. This experiment was successfully repeated three times.

Photometry Data Analysis

In vitro photometric data were acquired in Clampex 9 and initially analyzed using Clampfit v9 or v10 (Axon Instruments/Molecular Devices), exported to Excel for organization, and plotted and analyzed in GraphPad Prism 7. The PMT readout was offset corrected to zero (with the shutter closed) before basal fluorescence (F_0) and stimulation-induced increases in fluorescence (dF) values were obtained. Most photometric data are presented as dF/F_0 values to compensate for differences in basal fluorescence or dLight expression differences between slices. Voltammetric data were acquired in DEMON Voltammetry Software suite (Yorgason et al., 2011), exported to Excel for organization, and plotted and analyzed in GraphPad Prism 9.

In vivo fiber photometry data were collected using the SPCM64 9.8 Software (Becker & Hickl). The raw photon counts were exported in ascii format for analysis with custom Python or MATLAB scripts. Briefly, the fluorescence (F_{raw}) values were plotted as a function of time. Then, these fluorescence time series were converted to dF/F_0 in two ways. For the segmented photometry data (60-s per individual trial) obtained from operant conditioning sessions, F_0 was set to a moving average of each point with +/-15s sliding window similar to previously published methods (Patriarchi et al., 2018). Therefore, the baseline was normalized across all measurements such that only phasic dopamine transients were quantified. Occasionally, there was a negligible bleaching effect (<0.1% of F_0 degradation) within the 60-s of acquisition in our measurement setup even without the moving average normalization. For the continuous photometry measurements over 1-hr duration in the *in vivo* pharmacology experiments, the F_0 was estimated by a curve fitting method. We first validated that the degradation of fluorescence intensity was well predicted by an exponential decaying model. For this validation, we used control mice virally transduced to express GFP in dorsal striatum and dLight expressing mice having no drug injection to confirm the baseline prediction method. Then, for the actual experimental animals with cocaine and saline injections, the baseline curves of F_0 were estimated from the initial 20-min baseline measurement prior to the i.p. injection. Once the F_0 baseline was estimated, dF/F_0 was calculated using the standard method, in which $dF = F_{raw}-F_0$ and F_0 is the predicted baseline by exponential curve fitting.

Dopamine Transient Decay Analysis

For each CS+ trial, maximum peak location was identified using custom Matlab code. Then the fluorescence profile (dF/F) was normalized to the maximum intensity. The data points following the maximum intensity peak were fit using a double exponential decay model. In the fitted curve, the time point where the normalized fluorescence profile passed under 36.8% of the maximum intensity was selected as the transient decay time (or lifetime) of the phasic dopamine activity in each brain regions.

Drugs and Reagents

Cocaine-HCl was obtained from the National Institute on Drug Abuse. Dihydro-β-erythroidine hydrobromide (DHBE), nomifensine, quinpirole-HCl, and SCH23390 were purchased from Tocris Bioscience. Dopamine-HCl was purchased from Sigma Aldrich. All drugs were dissolved in ACSF. All other drugs and reagents, unless otherwise indicated, were obtained from Sigma Aldrich.

Statistics

GraphPad Prism 9.2 was used for all data analysis and statistics. For I-O curve comparison, two way ANOVA (method and stimulation intensity) was used. For the analysis of the caspase lesion curves, a mixed effects model was used (genotype and stimulation intensity factors). For the quinpirole inhibition and high calcium experiments, unpaired two-tailed t-tests were used. For data comparing *in vivo* transient amplitude, frequency, and decay constant changes, unpaired two-tailed t-tests were used. For analysis of the dorsal striatum subregion changes in decay constant, one way ANOVA was used. Unless otherwise indicated, all data represent the mean ± SEM.

Acknowledgements

We would like to thank Dr. Huaibin Cai for the Casp3 virus, Dr. Joseph Cheer for his comments on the data and manuscript, and Jacob Nadel and Lucas Voyvodic for their expert technical assistance with stereotaxic virus infusions. We also thank Rong Ye and Kevin Yu of the Confocal and Electron Microscopy Core, NIDA IRP, for collecting confocal and immune-electron microscopic images used in this study.

This work was supported by research grants from the National Institute on Alcohol Abuse and Alcoholism (K99R00 AA025991 to AGS, K99R00 AA027740 to SMA, and ZIA AA000407 & ZIA000416 to DML), the Intramural Research Program of the National Institute on Drug Abuse, the BRAIN Initiative (U01NS090604 and U01NS013522 to LT), and the National Institutes of Health (DP2MH107056 to LT).

Author Contributions

Designed Research: AGS, MM, YM, DML

Contributed Essential Reagents: TP, LT

Performed Research: AGS, YM, JOL, SMA, SZ

Analyzed Data: AGS, YM, JOL, SMA, SZ, MM

Wrote the Paper: AGS, YM, DML

Competing Interests

The authors declare no competing interests.

Bibliography

Beeler JA, Daw N, Frazier CR, Zhuang X (2010) Tonic dopamine modulates exploitation of reward learning. Front Behav Neurosci 4:170.

Berke JD (2018) What does dopamine mean? Nat Neurosci 21:787-793.

Brown HD, McCutcheon JE, Cone JJ, Ragozzino ME, Roitman MF (2011) Primary food reward and reward-predictive stimuli evoke different patterns of phasic dopamine signaling throughout the striatum. Eur J Neurosci 34:1997-2006.

Budygin EA, John CE, Mateo Y, Jones SR (2002) Lack of cocaine effect on dopamine clearance in the core and shell of the nucleus accumbens of dopamine transporter knock-out mice. J Neurosci 22:RC222.

Cachope R, Mateo Y, Mathur BN, Irving J, Wang HL, Morales M, Lovinger DM, Cheer JF (2012) Selective activation of cholinergic interneurons enhances accumbal phasic dopamine release: setting the tone for reward processing. Cell Rep 2:33-41.

Calabresi P, Mercuri NB, Di Filippo M (2009) Synaptic plasticity, dopamine and Parkinson's disease: one step ahead. Brain 132:285-287.

Calipari ES, Huggins KN, Mathews TA, Jones SR (2012) Conserved dorsal-ventral gradient of dopamine release and uptake rate in mice, rats and rhesus macaques. Neurochem Int 61:986-991.

Chefer VI, Thompson AC, Zapata A, Shippenberg TS (2009) Overview of brain microdialysis. Curr Protoc Neurosci Chapter 7:Unit7 1.

Church WH, Justice JB, Jr., Byrd LD (1987) Extracellular dopamine in rat striatum following uptake inhibition by cocaine, nomifensine and benztropine. Eur J Pharmacol 139:345-348.

Condon AF, Robinson BG, Asad N, Dore TM, Tian L, Williams JT (2021) The residence of synaptically released dopamine on D2 autoreceptors. Cell Rep 36:109465.

Covey DP, Roitman MF, Garris PA (2014) Illicit dopamine transients: reconciling actions of abused drugs. Trends Neurosci 37:200-210.

Cragg SJ, Rice ME (2004) DAncing past the DAT at a DA synapse. Trends Neurosci 27:270-277.

Feng J, Zhang C, Lischinsky JE, Jing M, Zhou J, Wang H, Zhang Y, Dong A, Wu Z, Wu H, Chen W, Zhang P, Zou J, Hires SA, Zhu JJ, Cui G, Lin D, Du J, Li Y (2019) A Genetically Encoded Fluorescent Sensor for Rapid and Specific In Vivo Detection of Norepinephrine. Neuron 102:745-761 e748.

Ford CP, Phillips PE, Williams JT (2009) The time course of dopamine transmission in the ventral tegmental area. J Neurosci 29:13344-13352.

Giros B, Jaber M, Jones SR, Wightman RM, Caron MG (1996) Hyperlocomotion and indifference to cocaine and amphetamine in mice lacking the dopamine transporter. Nature 379:606-612.

Grace AA (2016) Dysregulation of the dopamine system in the pathophysiology of schizophrenia and depression. Nat Rev Neurosci 17:524-532.

Graves SM, Surmeier DJ (2019) Delayed Spine Pruning of Direct Pathway Spiny Projection Neurons in a Mouse Model of Parkinson's Disease. Front Cell Neurosci 13:32.

Hamid AA, Pettibone JR, Mabrouk OS, Hetrick VL, Schmidt R, Vander Weele CM, Kennedy RT, Aragona BJ, Berke JD (2016) Mesolimbic dopamine signals the value of work. Nat Neurosci 19:117-126.

Hoffman AF, Spivak CE, Lupica CR (2016) Enhanced Dopamine Release by Dopamine Transport Inhibitors Described by a Restricted Diffusion Model and Fast-Scan Cyclic Voltammetry. ACS Chem Neurosci 7:700-709.

Hurd YL, Kehr J, Ungerstedt U (1988) In vivo microdialysis as a technique to monitor drug transport: correlation of extracellular cocaine levels and dopamine overflow in the rat brain. J Neurochem 51:1314-1316.

Hyland BI, Reynolds JN, Hay J, Perk CG, Miller R (2002) Firing modes of midbrain dopamine cells in the freely moving rat. Neuroscience 114:475-492.

Jones SR, Gainetdinov RR, Jaber M, Giros B, Wightman RM, Caron MG (1998) Profound neuronal plasticity in response to inactivation of the dopamine transporter. Proc Natl Acad Sci U S A 95:4029-4034.

Kile BM, Guillot TS, Venton BJ, Wetsel WC, Augustine GJ, Wightman RM (2010) Synapsins differentially control dopamine and serotonin release. J Neurosci 30:9762-9770.

Kishida KT, Sandberg SG, Lohrenz T, Comair YG, Saez I, Phillips PE, Montague PR (2011) Sub-second dopamine detection in human striatum. PLoS One 6:e23291.

Kupferschmidt DA, Juczewski K, Cui G, Johnson KA, Lovinger DM (2017) Parallel, but Dissociable, Processing in Discrete Corticostriatal Inputs Encodes Skill Learning. Neuron 96:476-489 e475.

Labouesse MA, Cola RB, Patriarchi T (2020) GPCR-Based Dopamine Sensors-A Detailed Guide to Inform Sensor Choice for In vivo Imaging. Int J Mol Sci 21.

Liu C, Goel P, Kaeser PS (2021) Spatial and temporal scales of dopamine transmission. Nat Rev Neurosci 22:345-358.

Lohani S, Martig AK, Underhill SM, DeFrancesco A, Roberts MJ, Rinaman L, Amara S, Moghaddam B (2018) Burst activation of dopamine neurons produces prolonged post-burst availability of actively released dopamine. Neuropsychopharmacology 43:2083-2092.

Mamaligas AA, Cai Y, Ford CP (2016) Nicotinic and opioid receptor regulation of striatal dopamine D2-receptor mediated transmission. Sci Rep 6:37834.

Marcott PF, Mamaligas AA, Ford CP (2014) Phasic dopamine release drives rapid activation of striatal D2-receptors. Neuron 84:164-176.

Martel JC, Gatti McArthur S (2020) Dopamine Receptor Subtypes, Physiology and Pharmacology: New Ligands and Concepts in Schizophrenia. Front Pharmacol 11:1003.

Mateo Y, Budygin EA, John CE, Banks ML, Jones SR (2004) Voltammetric assessment of dopamine clearance in the absence of the dopamine transporter: no contribution of other transporters in core or shell of nucleus accumbens. J Neurosci Methods 140:183-187.

Mohebi A, Pettibone JR, Hamid AA, Wong JT, Vinson LT, Patriarchi T, Tian L, Kennedy RT, Berke JD (2019) Dissociable dopamine dynamics for learning and motivation. Nature 570:65-70.

Nestler EJ, Carlezon WA, Jr. (2006) The mesolimbic dopamine reward circuit in depression. Biol Psychiatry 59:1151-1159.

Oleson EB, Salek J, Bonin KD, Jones SR, Budygin EA (2009) Real-time voltammetric detection of cocaine-induced dopamine changes in the striatum of freely moving mice. Neurosci Lett 467:144-146.

Ott T, Nieder A (2019) Dopamine and Cognitive Control in Prefrontal Cortex. Trends Cogn Sci 23:213-234.

Patriarchi T, Mohebi A, Sun J, Marley A, Liang R, Dong C, Puhger K, Mizuno GO, Davis CM, Wiltgen B, von Zastrow M, Berke JD, Tian L (2020) An expanded palette of dopamine sensors for multiplex imaging in vivo. Nat Methods 17:1147-1155.

Patriarchi T, Cho JR, Merten K, Howe MW, Marley A, Xiong WH, Folk RW, Broussard GJ, Liang R, Jang MJ, Zhong H, Dombeck D, von Zastrow M, Nimmerjahn A, Gradinaru V, Williams JT, Tian L (2018) Ultrafast neuronal imaging of dopamine dynamics with designed genetically encoded sensors. Science 360.

Richfield EK, Young AB, Penney JB (1989) Comparative distributions of dopamine D-1 and D-2 receptors in the cerebral cortex of rats, cats, and monkeys. J Comp Neurol 286:409-426.

Sabatini BL, Tian L (2020) Imaging Neurotransmitter and Neuromodulator Dynamics In Vivo with Genetically Encoded Indicators. Neuron 108:17-32.

Salinas AG, Davis MI, Lovinger DM, Mateo Y (2016) Dopamine dynamics and cocaine sensitivity differ between striosome and matrix compartments of the striatum. Neuropharmacology 108:275-283.

Salinas AG, Mateo Y, Carlson VCC, Stinnett GS, Luo G, Seasholtz AF, Grant KA, Lovinger DM (2021) Long-term alcohol consumption alters dorsal striatal dopamine release and regulation by D2 dopamine receptors in rhesus macaques. Neuropsychopharmacology 46:1432-1441.

Sgobio C, Sun L, Ding J, Herms J, Lovinger DM, Cai H (2019) Unbalanced calcium channel activity underlies selective vulnerability of nigrostriatal dopaminergic terminals in Parkinsonian mice. Sci Rep 9:4857.

Sgobio C, Kupferschmidt DA, Cui G, Sun L, Li Z, Cai H, Lovinger DM (2014) Optogenetic measurement of presynaptic calcium transients using conditional genetically encoded calcium indicator expression in dopaminergic neurons. PLoS One 9:e111749.

Sun F et al. (2018) A Genetically Encoded Fluorescent Sensor Enables Rapid and Specific Detection of Dopamine in Flies, Fish, and Mice. Cell 174:481-496 e419.

Surmeier DJ, Graves SM, Shen W (2014) Dopaminergic modulation of striatal networks in health and Parkinson's disease. Curr Opin Neurobiol 29:109-117.

Threlfell S, Lalic T, Platt NJ, Jennings KA, Deisseroth K, Cragg SJ (2012) Striatal dopamine release is triggered by synchronized activity in cholinergic interneurons. Neuron 75:58-64.

Unger EK et al. (2020) Directed Evolution of a Selective and Sensitive Serotonin Sensor via Machine Learning. Cell 183:1986-2002 e1926.

Venton BJ, Cao Q (2020) Fundamentals of fast-scan cyclic voltammetry for dopamine detection. Analyst 145:1158-1168.

Venton BJ, Zhang H, Garris PA, Phillips PE, Sulzer D, Wightman RM (2003) Real-time decoding of dopamine concentration changes in the caudate-putamen during tonic and phasic firing. J Neurochem 87:1284-1295.

Venton BJ, Seipel AT, Phillips PE, Wetsel WC, Gitler D, Greengard P, Augustine GJ, Wightman RM (2006) Cocaine increases dopamine release by mobilization of a synapsin-dependent reserve pool. J Neurosci 26:3206-3209.

Wang Q, Zhang W (2016) Maladaptive Synaptic Plasticity in L-DOPA-Induced Dyskinesia. Front Neural Circuits 10:105.

Wang Y, Toyoshima O, Kunimatsu J, Yamada H, Matsumoto M (2021) Tonic firing mode of midbrain dopamine neurons continuously tracks reward values changing moment-by-moment. Elife 10.

Willuhn I, Burgeno LM, Everitt BJ, Phillips PE (2012) Hierarchical recruitment of phasic dopamine signaling in the striatum during the progression of cocaine use. Proc Natl Acad Sci U S A 109:20703-20708.

Wu Q, Reith ME, Kuhar MJ, Carroll FI, Garris PA (2001) Preferential increases in nucleus accumbens dopamine after systemic cocaine administration are caused by unique characteristics of dopamine neurotransmission. J Neurosci 21:6338-6347.

Yorgason JT, Espana RA, Jones SR (2011) Demon voltammetry and analysis software: analysis of cocaine-induced alterations in dopamine signaling using multiple kinetic measures. J Neurosci Methods 202:158-164.

Zhai S, Tanimura A, Graves SM, Shen W, Surmeier DJ (2018) Striatal synapses, circuits, and Parkinson's disease. Curr Opin Neurobiol 48:9-16.

Zhang S, Qi J, Li X, Wang HL, Britt JP, Hoffman AF, Bonci A, Lupica CR, Morales M (2015) Dopaminergic and glutamatergic microdomains in a subset of rodent mesoaccumbens axons. Nat Neurosci 18:386-392.

Zhou FM, Liang Y, Dani JA (2001) Endogenous nicotinic cholinergic activity regulates dopamine release in the striatum. Nat Neurosci 4:1224-1229.

Figure Legends

Figure 1. Simultaneous comparison of dLight and FSCV dopamine responses in dorsal striatum. (a) Schematic of simultaneous dLight photometric and FSCV recordings. (b) dLight signal is completely blocked by application of the D1 dopamine receptor antagonist, SCH23390. (c) Input-output curves directly comparing dLight photometric and FSCV DA measurements. (d) Schematic illustrating the viral strategy used to ablate substantia nigra DA neurons to confirm that changes in striatal dLight fluorescence are due to dopamine. (e & f) Genetic ablation of nigral DA neurons results in markedly reduced dopamine release measured with dLight and FSCV. Representative traces (g) and summarized data (h) showing that application of the D2 dopamine receptor agonist, quinpirole, activates presynaptic D2 autoreceptors on dopamine axons to inhibit dopamine release equally with both methods. (i & j) Increasing extracellular calcium increased dLight fluorescent responses. * $p<0.05$, ** $p<0.01$. Error bars represent the SEM.

Figure 2. DAT blockers do not increase DA release. (a) Representative traces of simultaneously collected dLight (blue shades) and FSCV (orange shades) DA transients before and after application of cocaine. (b) Summary data showing that application of cocaine to dorsal striatal slices dose dependently increases peak DA transient height with FSCV but not dLight photometry methods. (c) Summary data showing that DA transient duration is increased with both methods following cocaine application. Similarly, the specific DAT inhibitor, nomifensine (1 μM) increases DA transient peak height with FSCV but not dLight photometry measurements (d). (e) Cocaine does not increase DA transient peak height in DAT KO mice. (f-h) Modifying the typical FSCV waveform to change the adsorption properties alters the effects of DAT blockade with 1 μM nomifensine. (i) Schematic of model for DAT inhibitor-induced increases in dopamine transient peak height in FSCV. Error bars represent the SEM.

Figure 3. Dorsal striatum expression of dLight sensor on plasma membrane of dendrites synapsing with TH-axons. Immunofluorescence detection of dLight-GFP sensor (green) and TH (red) in the dorsal striatum from a mouse injected with a viral vector encoding dLight sensor tethered to GFP (a). Apposition of a dLight-GFP-positive dendrite and TH-positive axon is seen at high magnification (right panels). (b) Electron micrographs of immunogold detection of dLight-GFP sensor (gold particles, green arrowheads) on the plasma membrane of a dendrite (green outline in b). Note the apposition of dendritic dLight-GFP and a presynaptic axon (blue arrow in b). (c) dLight-GFP expression on the plasma membrane of a soma (green outline). Note also the dLight-GFP sensor (gold particles) in association with Golgi apparatus and endoplasmic reticulum (ER). (d) Detection of dLight-GFP sensor (scattered dark material, green arrowheads) in a dendrite (green outline) establishing synapses (blue arrows) with a TH- positive axon (gold particles, red arrowheads).

Figure 4. *In vivo* DA measurement in DLS following cocaine administration. (a) Schematic of in vivo fiber photometry system. (b) Sample fluorescence (dF/F, % baseline) profile of DA activity in DLS following i.p. cocaine injection. (c) Average fluorescence (dF/F, normalized to session maximum) profile of DA activity in DLS following i.p. cocaine injection (n=4). (d) Magnified dF/F profile illustrating DA activity before (Baseline) and after i.p. cocaine injection. (e) Averaged

fluorescence (dF/F, normalized to session maximum) profile of baseline DA transients, time-locked to the transient peaks (n=64). (f) Averaged fluorescence (dF/F, normalized to session maximum) profile of DA transients following cocaine injection, time-locked to the transient peaks (n=165). DA transient frequency (g) and amplitude (h) were increased following cocaine injection. Each point denotes a five minute average. (i) Average exponential fit of normalized dopamine transient decay. (j) Fitted exponential decay constant values showing longer DA transient decay time following cocaine injection; individual points correspond to individual transients. (k) dLight fluorescence is blocked by in vivo administration of the D1R antagonist, SCH23390. (l) Representative dF/F profiles for dLight in DLS before and after SCH23390 administration as well as for an eGFP control mouse. *** $p<0.001$. Shaded areas and error bars represent the SEM.

Figure 5. *In vivo* DA dynamics across striatal regions during Pavlovian training. (a) Schematic of the experimental design and measurement sites (b). (c) Average dF/F profiles of dLight activity in NAc, DMS, and DLS mid-training. (d) Averaged decay constant fitting of normalized DA transients aligned to the onset of CS+ (e) Summarized decay constants across striatal regions, each point is a session average with a minimum of 15 CS+ trials per session, 5 sessions per each animal, total 6 mice (one-way ANOVA with Bonferroni's correction for multiple comparisons, **** $p<0.0001$). (f) Across striatal regions, DA responses to CS+ and reward (top row) and CS- responses (bottom row). (g) Long-term measurement of DA transients in DLS across 10 weeks of training. (h) long-lasting CS+ and reward associated DA responses in DLS. * $p<0.05$. Error bars and shaded areas represent the SEM.

Figure 1

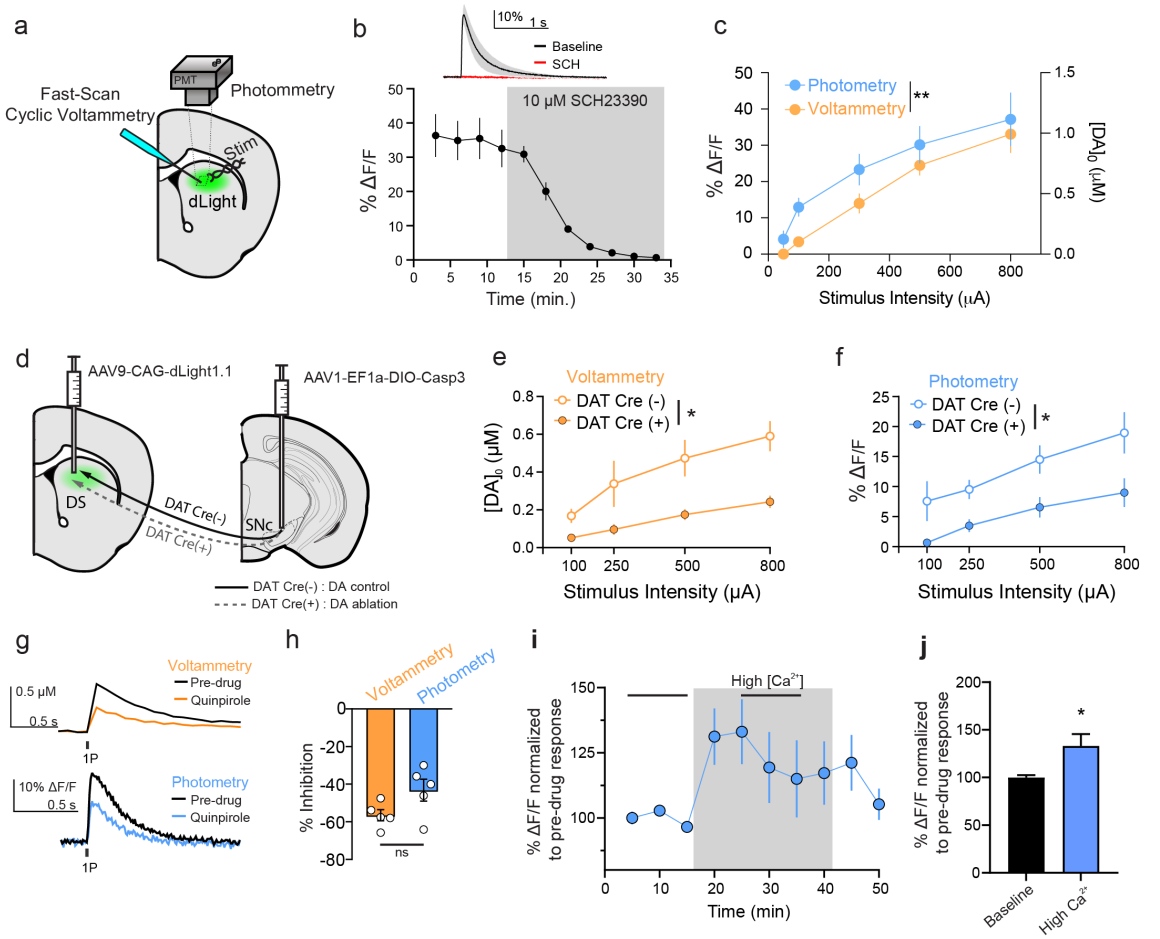

Figure 2

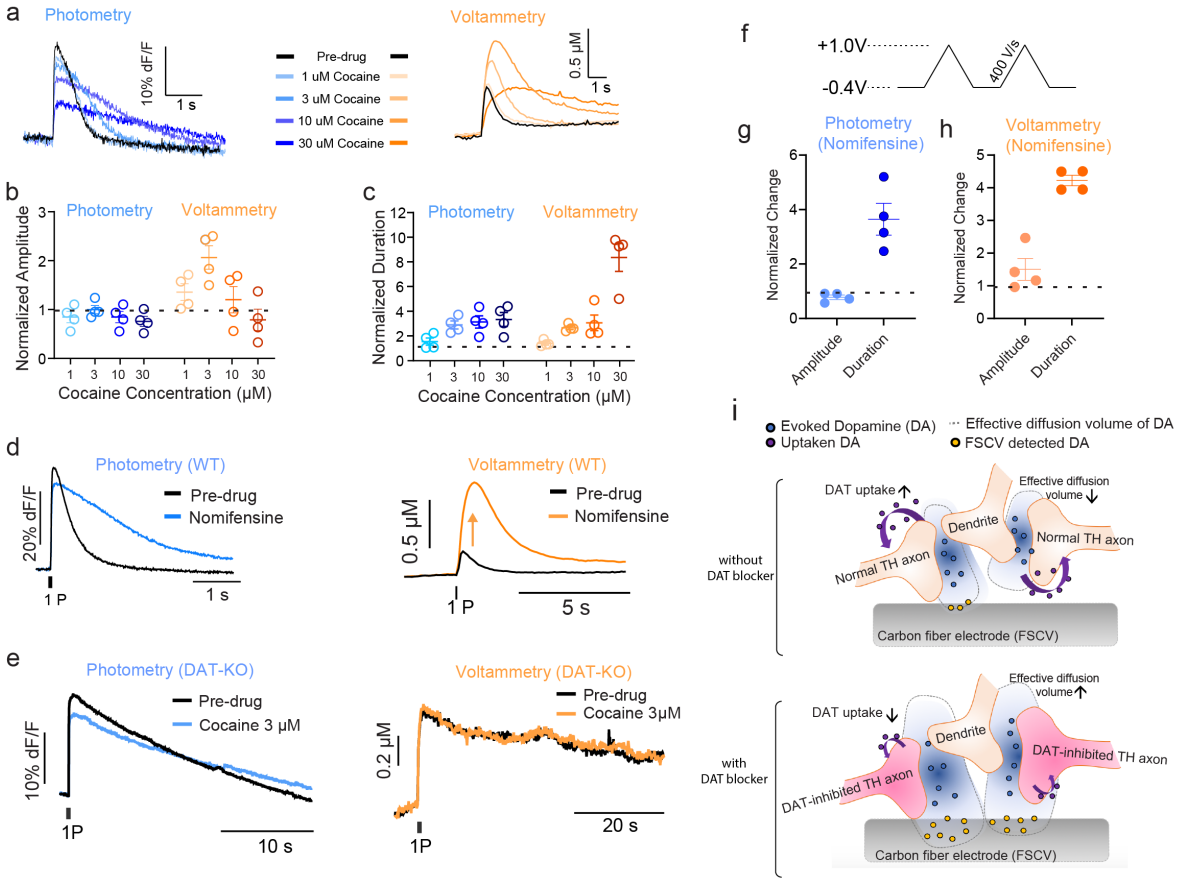

Figure 3

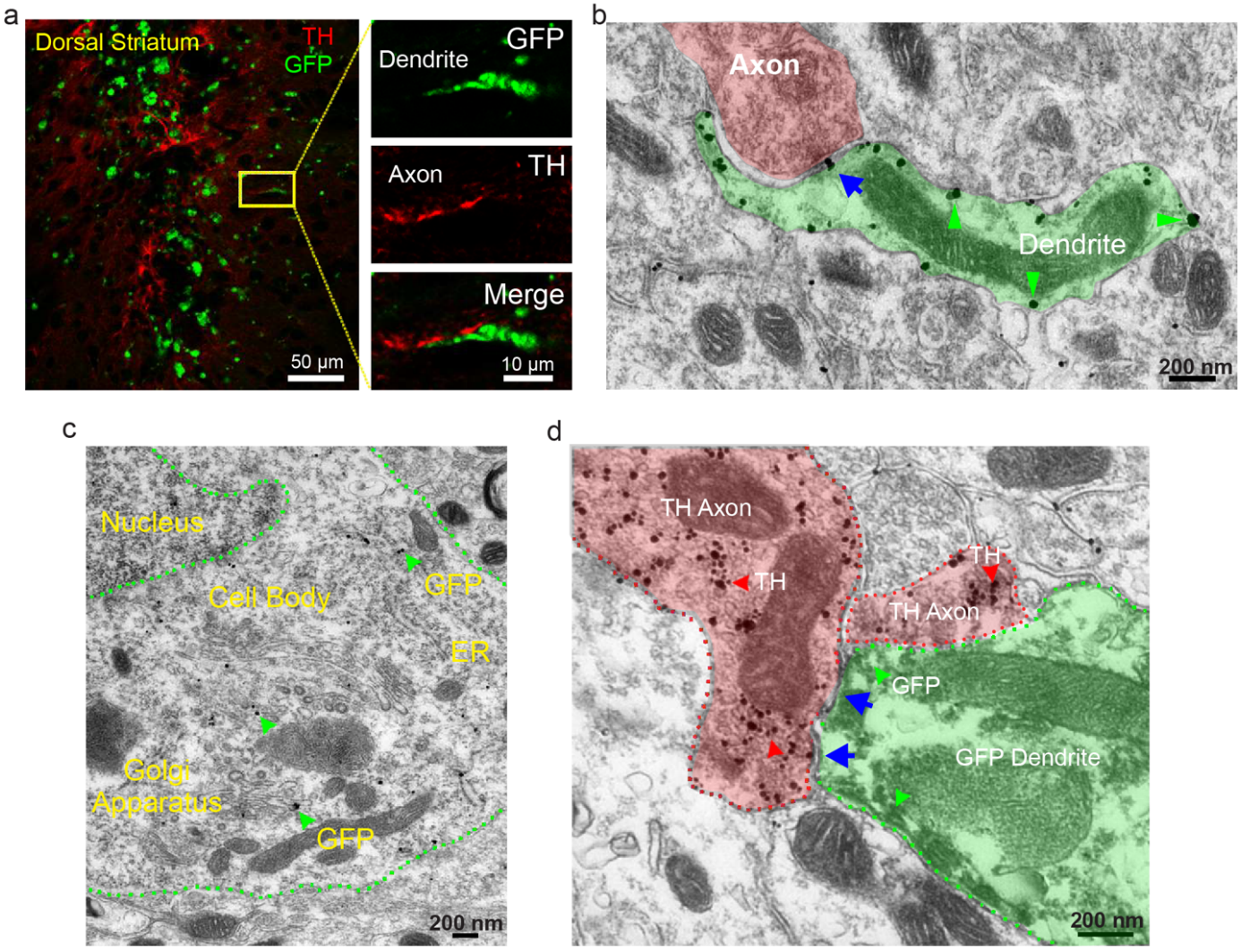

Figure 4

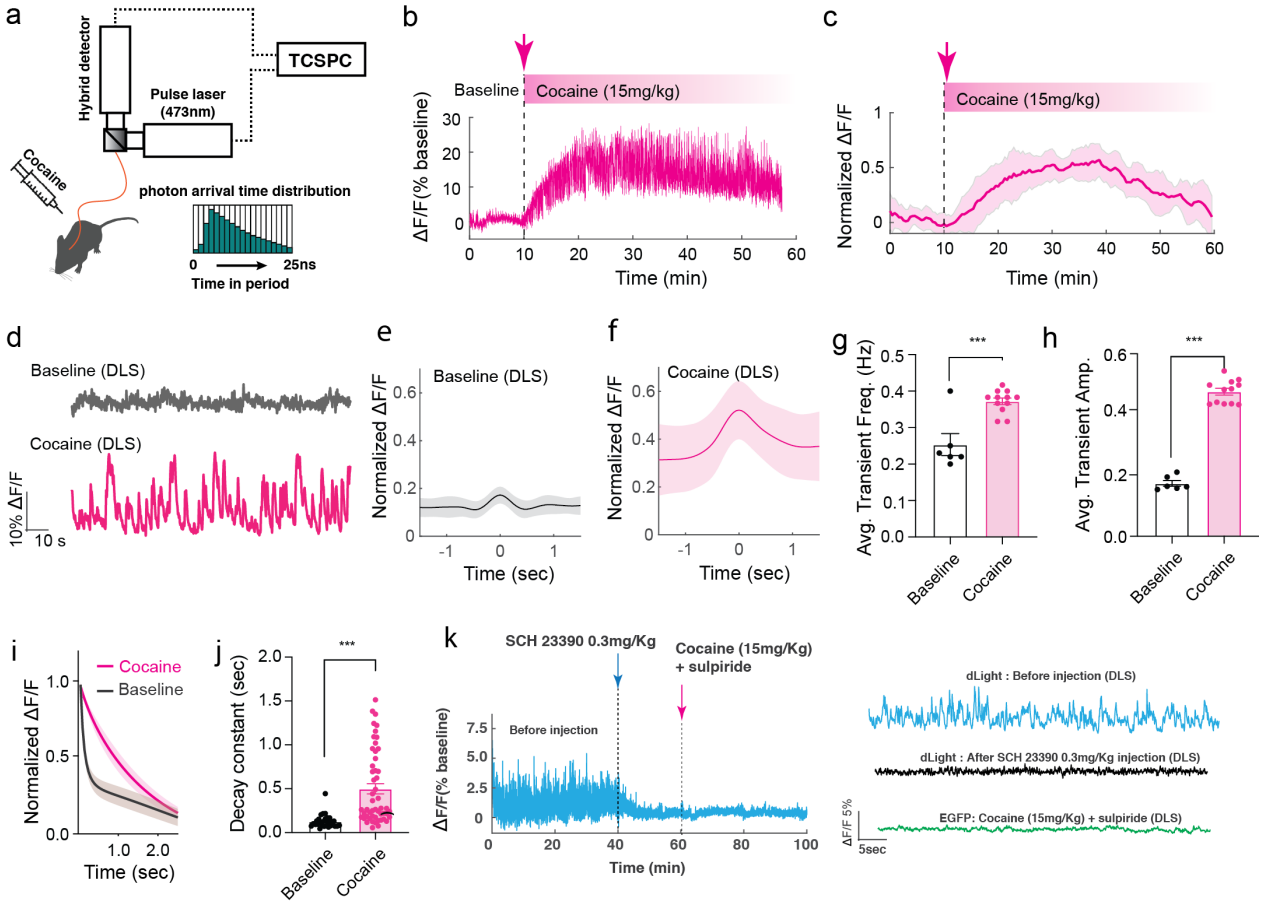

Figure 5